

RESEARCH ARTICLE

Bilateral flight muscle activity predicts wing kinematics and 3-dimensional body orientation of locusts responding to looming objects

Glyn A. McMillan, Vicky Loessin and John R. Gray*

Department of Biology, 112 Science Place, University of Saskatchewan, Saskatoon, SK, Canada S7N 5E2

*Author for correspondence (jack.gray@usask.ca)

SUMMARY

We placed locusts in a wind tunnel using a loose tether design that allowed for motion in all three rotational degrees of freedom during presentation of a computer-generated looming disc. High-speed video allowed us to extract wing kinematics, abdomen position and 3-dimensional body orientation. Concurrent electromyographic (EMG) recordings monitored bilateral activity from the first basalar depressor muscles (m97) of the forewings, which are implicated in flight steering. Behavioural responses to a looming disc included cessation of flight (wings folded over the body), glides and active steering during sustained flight in addition to a decrease and increase in wingbeat frequency prior to and during, respectively, an evasive turn. Active steering involved shifts in bilateral m97 timing, wing asymmetries and whole-body rotations in the yaw (ψ), pitch (χ) and roll (η) planes. Changes in abdomen position and hindwing asymmetries occurred after turns were initiated. Forewing asymmetry and changes in η were most highly correlated with m97 spike latency. Correlations also increased as the disc approached, peaking prior to collision. On the inside of a turn, m97 spikes occurred earlier relative to forewing stroke reversal and bilateral timing corresponded to forewing asymmetry as well as changes in whole-body rotation. Double spikes in each m97 occurred most frequently at or immediately prior to the time the locusts turned, suggesting a behavioural significance. These data provide information on mechanisms underlying 3-dimensional flight manoeuvres and will be used to drive a closed loop flight simulator to study responses of motion-sensitive visual neurons during production of realistic behaviours.

Supplementary material available online at <http://jeb.biologists.org/cgi/content/full/216/17/3369/DC1>

Key words: *Locusta migratoria*, insect flight, loom, collision avoidance, motor control.

Received 4 March 2013; Accepted 14 May 2013

INTRODUCTION

Flying animals are particularly challenged with producing coordinated escape behaviours. Generating appropriate aerodynamic forces while staying aloft requires rapid detection and integration of salient visual cues. Animals have evolved neural circuitry adapted to preferentially detect visual edge expansion of looming stimuli and respond accordingly by generating emergency escape behaviours [for example, frogs (Nakagawa and Hongjian, 2010), cats (Liu et al., 2011), pigeons (Wang and Frost, 1992), crabs (Oliva et al., 2007; Sztarker and Tomsic, 2008) and insects such as flies (Holmqvist and Srinivasan, 1991; Fotowat et al., 2009) and locusts (Robertson and Reye, 1992; Robertson and Johnson, 1993; Gray et al., 2001; Santer et al., 2005; Simmons et al., 2010; Fotowat et al., 2011; Chan and Gabbiani, 2013)].

Locusts respond to looming stimuli by performing subtle movements of their appendages to hide behind a blade of grass (Hassenstein and Huster, 1999), kicking and jumping (Burrows and Rowell, 1973; Burrows, 1995), or turning and gliding during flight (Robertson and Reye, 1992; Robertson and Johnson, 1993; Gray et al., 2001; Santer et al., 2005; Simmons et al., 2010; Chan and Gabbiani, 2013). While flying in dense swarms and avoiding collisions with conspecifics, locusts must also escape potential aerial predators (Waloff, 1972; Santer et al., 2012). This type of aerobatic control is largely influenced by the locust's visual system (Gray et al., 2001; Santer et al., 2005; Santer et al., 2006), which contains multiple looming-sensitive neurons that synapse with flight motor neurons in the thorax (Simmons, 1980).

To date, flight muscle activity, wing kinematics and aerodynamic forces recorded during a collision avoidance behaviour have been measured from rigidly tethered locusts flying in open-loop conditions (Robertson and Reye, 1992; Robertson and Johnson, 1993; Hedwig and Becher, 1998; Gray et al., 2001; Santer et al., 2005; Santer et al., 2006; Simmons et al., 2010; Ribak et al., 2012), which introduces potentially confounding artefacts (Robertson and Reye, 1992; Dawson et al., 2004a; Shoemaker and Robertson, 1998). However, loosely tethered flying locusts are capable of changing orientation in response to looming stimuli within a single wing beat (Mohr and Gray, 2003). Using a modified rigid tether, Ribak and colleagues (Ribak et al., 2012) showed that locusts generated avoidance responses (roll) within a single downstroke. A more complete understanding of locust flight steering requires that animals be allowed to manoeuvre in 3-dimensional space, under closed-loop feedback conditions. Recently, using minimally restrained flying locusts, Chan and Gabbiani (Chan and Gabbiani, 2013) observed a variety of behaviours that have been previously shown (or indicated) to occur in tethered preparations. While they described wing kinematics and body rotations (ψ and χ) using a more restrained preparation, they did not describe changes in other components of steering, such as leg and abdomen movement, and changes in wingbeat frequency. We used a combination of electromyographic (EMG) recordings and motion analysis to show relationships between forewing depressor muscle activity, wing kinematics and 3-dimensional body orientation of flying locusts responding to lateral looming visual stimuli.

MATERIALS AND METHODS

Animals

Experiments were performed on 18 adult male *Locusta migratoria* (Linnaeus 1758) selected at least 3 weeks past the imaginal moult from a crowded colony (25–28°C, 12h:12h light:dark cycle) maintained at the University of Saskatchewan in Saskatoon, Canada. Experiments were carried out at room temperature (~25°C) during similar times of the animals' light cycle to eliminate potential variation in responsiveness known to occur when locusts fly at night (Gaten et al., 2012).

Preparation

The locust's legs were removed to prevent the EMG electrodes from being dislodged (Robertson et al., 1996). A ringed tether was mounted onto the dorsum of the pronotum using low melting point beeswax and the locust was then rotated ventral side up. Two single 100 μ m fine copper EMG wires (Belden, St Laurent, QB, Canada) that were insulated except at the tip were inserted into the left and right forewing first basalar depressor muscles (m97) and the ground was inserted slightly off the midline of the mesothoracic sternum. In rigidly tethered locusts, bilateral m97 timing is associated with attempted steering manoeuvres (Möhl and Zarnack, 1977a; Zarnack, 1988; Dawson et al., 1997; Shoemaker and Robertson, 1998; Dawson et al., 2004b). The EMG wires were held in place with low melting point beeswax. The tether consisted of 45 cm of 0.2 mm diameter, clear fishing line (Berkley Trilene XT Extra Tough Line, Pure Fishing, Columbia, SC, USA; 0.02 g) attached to the top of a 1.2 cm (outer diameter) metal electrical ring connector (0.64 g) with markings at the top, bottom, left and right quadrants (Fig. 1B). The total mass of the tether, wax (0.02 g) and EMG wires (0.08 g) was 0.76 g. Fully intact locusts weighed ~2 g (range 1.8–2.5 g) and ~1.67 g with legs (~0.33 g) removed. Therefore, accounting for removal of the legs, locusts carried an additional 0.43 g (~20%) above their fully intact mass.

The locust was suspended 45 cm from the upwind end and in the centre of the cross-section of a 0.9×0.9×3 m Plexiglas wind tunnel. This positioning placed the locust 45 cm from the rear projection screen that was mounted on the right side of the wind tunnel. Wind speed was set to 3 m s⁻¹, as measured with a hot-wire anemometer (VWR Scientific, Edmonton, AB, Canada), which is within the range of a locust's average natural flight speed (3–6 m s⁻¹) (Baker et al., 1981). Room lights were turned off during experimentation and the preparation was illuminated from above and behind using two 250 W halogen lights.

Visual stimuli

Visual stimuli began once locusts maintained >5 min of stable position within the wind stream (see supplementary material Movie 1). The stimulus was a computer-generated image of a 7 cm black disc approaching at 3 m s⁻¹ projected onto a rectangular rear-projection screen (96×63 cm) mounted on the right side of the wind tunnel (Fig. 1A). These parameters produced a ratio of the half size of the object (l) to the absolute approach velocity ($|v|$) of $l/|v|=12$ ms, which is consistent with values that represent known aerial predators of *L. migratoria* (Santer et al., 2012). The disc expanded along a trajectory perpendicular to the locust's longitudinal axis at 0 deg elevation and 90 deg azimuth such that the centre of the looming object directly approached the centre of the right eye. A Quantum Instruments PMLX photometer (B & H Photo, New York, NY, USA) placed at the projection screen was used to measure the luminance of the black disc (3.8 cd m⁻²) on the white background (36.4 cd m⁻²), producing a Michelson contrast ratio of 0.81. A

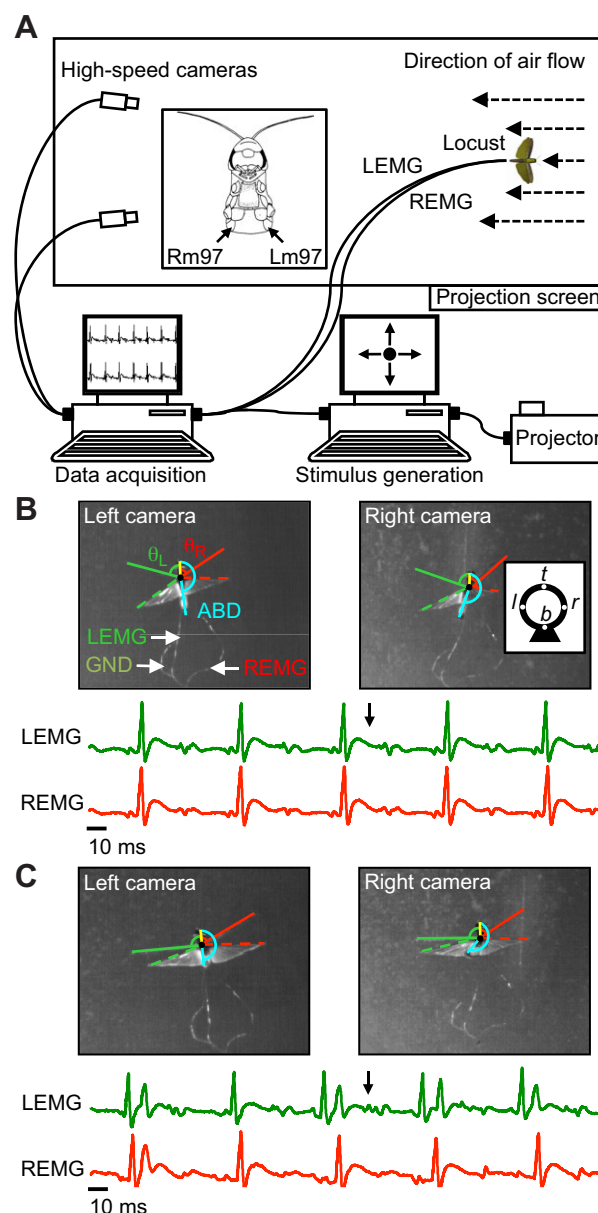


Fig. 1. Experimental setup used to record 3D flight kinematics and electromyographic (EMG) data. (A) Top view of the wind tunnel (0.9×0.9×3 m) equipped with two high-speed digital cameras (250 frames s⁻¹). The locust, with implanted EMG electrodes (inset), was suspended in the centre of the wind tunnel facing upstream of the air flow. A looming black 7 cm disc on a white background was projected onto a rear projection screen attached to the side of the wind tunnel (see supplementary material Movie 1). One computer was used for stimulus generation, while a second computer was used to synchronize and save behavioural flight data from the video cameras, video frames from the stimulus, vertical synchronization pulses from the projector, and EMG recordings from the left (L) and right (R) m97 muscles. (B) Time-aligned single frames from each camera recording the behaviour of one animal, and the concurrent left (L) and right (R) EMG activity, during straight flight. ABD, abdomen angle; GND, ground wire; θ_L , left wing angle; θ_R , right wing angle. The inset in the right camera frame is a schematic diagram of the tether coordinate system: t , top; r , right; b , bottom; l , left. Single, synchronized spikes from each muscle correspond to the top of symmetrical wing downstrokes. (C) Time-aligned single frames from each camera, recording behaviour of the same animal as in B, and concurrent EMG activity during a left turn. Earlier doublet LEMG spikes corresponded to greater depression of the left wing at the start of the downstroke. See Materials and methods for a description of angle normalization. Arrows associated with EMG traces indicate the time of the video frames.

1024×1024 pixel portable network graphics (png) file of a black disc was scaled on a white background and rendered at 85 frames s⁻¹, which is above the flicker fusion frequency of the locust eye (Miall, 1978), using VisionEgg visual stimulus generating software (Straw, 2008) running on a Python programming platform. Each looming stimulus lasted 4 s, starting at a virtual distance of 1200 cm and reaching a maximum size of 7 cm on the screen (subtending ~0.33 and ~9 deg, respectively of the locust's visual field). To ensure a smooth approach from a single point in space, the initial subtense angle was well below the acceptance angle of an individual ommatidium (~1 deg) (Horridge and McLean, 1978). Based on the position of the locust during stable flight [at x -, y -, z -coordinates (0,0,0)], the projected time of collision (TOC) occurred ~150 ms after the end of object motion. During straight flight, the locust's position deviated maximally ± 2.5 cm in the x -axis, ± 0.6 cm in the y -axis and ± 1 cm in the z -axis. Movements in the x -axis would thus have produced a variation in the TOC of ± 8 ms, which was relatively small compared with the variation in the range of turn reaction time (~760 ms). Therefore, TOC was calculated as the time the disc would have reached coordinates (0,0,0).

Recording techniques

Flight activity was recorded with two digital cameras (Motion Scope, Redlake Camera, San Diego, CA, USA), located behind the locust and 15 deg to either side of the midline of the wind tunnel (Fig. 1A). Each camera, recording at 250 frames s⁻¹, was connected to a separate PCI card that stored 8 s of data on the on-board RAM. Simultaneous EMG data were recorded continuously using two channels of an A/D converter (National Instruments, Vaudreuil-Dorion, QB, Canada) recording at 25,000 samples s⁻¹. To align video and physiological data with TOC, we embedded square-wave synchronization pulses within each rendered frame of a stimulus presentation. These pulses, along with the transistor–transistor logic (TTL) video signal from each frame of the video card were recorded on two separate A/D channels and used for offline analysis. Simultaneous video, physiological and time alignment data were synchronized and controlled using Midas 2.0 event capture software (Xcitex, Cambridge, MA, USA) (Fig. 2).

Data analysis

Video files for each camera from the same trial were imported into WinAnalyze3D motion analysis software (Mikromak, Berlin, Germany), which was calibrated for 3-dimensional measurements using a 32-point calibration frame. Adobe Premiere Pro CS6 (version 6.0.0, San Jose, CA, USA) was used to examine flight video and obtain times of behavioural changes. We defined behavioural responses to looming stimuli as a momentary cessation of wing activity (stop or glide), movement toward the stimulus (right turn) or movement away from the stimulus (left turn). Stops occurred when flapping flight ceased and the wings folded against the body of the locust. During a glide, the forewings were held above the hindwings at the top of their upstroke and hindwing movement stopped at the same time during the downstroke (Baker and Cooter, 1979). The glide is a stereotypical behavioural posture where the wings stop moving and remain elevated above the body until the wings move downwards and flapping flight resumes (Baker and Cooter, 1979; Santer et al., 2005). The end of a glide and stop is signalled by the resumption of flapping flight. The time of forewing stroke reversal prior to whole-body movement indicated the time of a turn (TOT). In the videos, it was possible to clearly see how the forewing positions correlated with the position of the locust in 3-dimensional space prior to a turn, often in a single wing beat. The

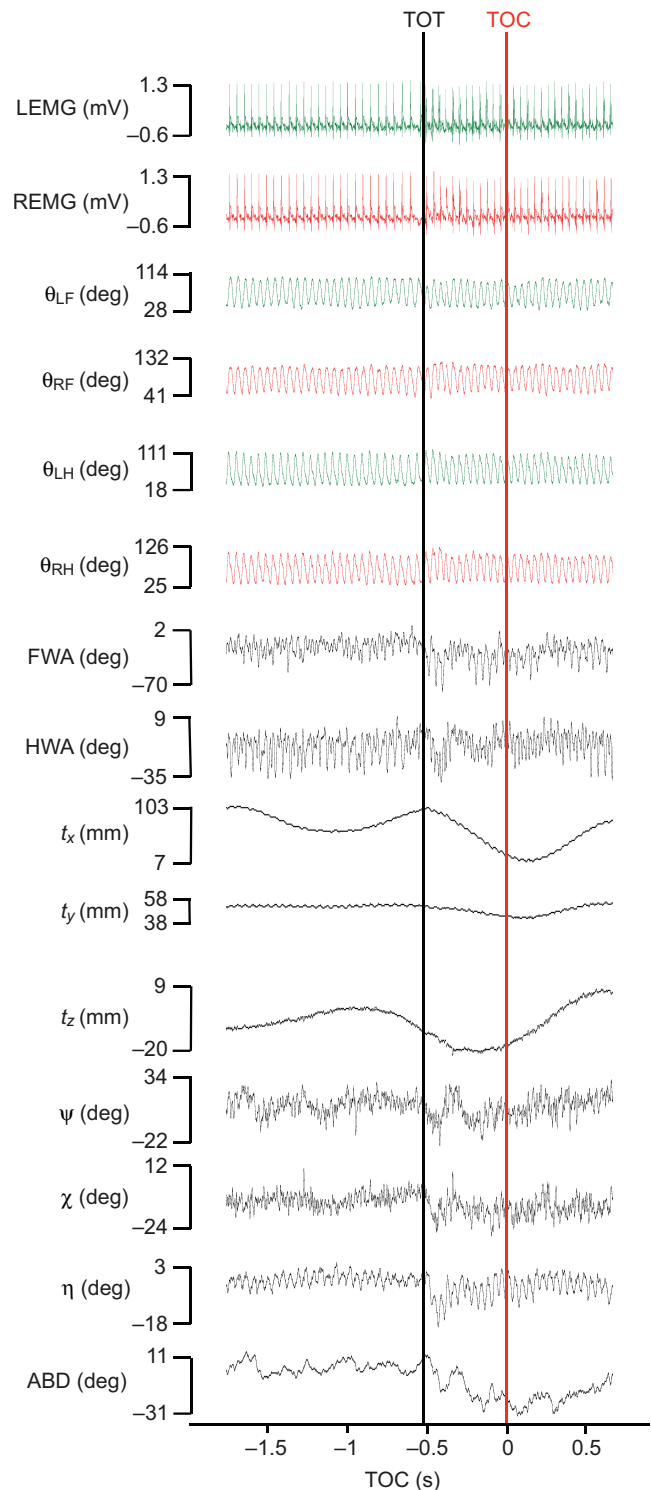


Fig. 2. Concurrent EMG, kinematic and body orientation data for one approach where the locust turned to the left (refer to supplementary material Movie 1 for visual representation). Data are aligned to the time of projected collision (TOC, red vertical line) of an expanding 7 cm disc. The left forewing angle (θ_{LF}), right forewing angle (θ_{RF}), left hindwing angle (θ_{LH}) and right hindwing angle (θ_{RH}) were used to calculate the forewing (FWA) and hindwing (HWA) asymmetries accordingly. Tether marks (t_x , t_y and t_z) represent changes in the x -, y - and z -planes for the top tether (bottom and side data not shown). Rotation angles in 3-dimensional space (yaw, ψ ; pitch, χ ; and roll, η) were calculated as described in Materials and methods (Eqn 1). TOT, time of turn (black vertical line). Units are provided on the right side of the figure and represent maximum and minimum values of the associated parameters.

times of each behaviour were correlated with kinematic and EMG recordings. In addition to the TOC, the TOT was also used as a reference time. Glide and stop duration were easier to quantify than turn duration, as the tether often caused a later fulcrum effect that swung the animals in the opposite direction of a turn. Therefore, the end of a turn occurred when the locusts reached the maximum length of the wire on the tether and began to move in the direction opposite to the initial turn direction. In some cases, the animal moved outside of the view of the cameras. We obtained x -, y - and z -coordinates from the top, right, bottom and left markers on the tether, the tips of the right and left forewings and hindwings, the posterior tip of the abdomen, and on the mesothorax between the base of the forewings in each video frame from each camera. These coordinates and the wing and abdomen position relative to the top of the disc and the thorax were imported into DataView (version 6.3.2, St Andrews, UK) and merged with files containing EMG recordings, trigger and synchronization information for the same stimulus presentation. Three-dimensional wing and abdomen angles were calculated in WinAnalyze and imported into DataView where event detection marked the top and bottom of each wing stroke. The top of the wing stroke was represented by a greater angle than the bottom of the wing stroke given that 0 deg was designated as being directly below the locust. The abdomen position was normalized to 180 deg relative to the midline of the locust such that a shift to the left provided a negative value and a shift to the right provided a positive value. The x -, y - and z -coordinates for the four marks on the tether were used to calculate the roll (η), pitch (χ) and yaw (ψ) angles of the locust during flight. η was calculated using the x - and y -coordinates for the top (t) and bottom (b) of the tether disc, where b_x is the x -coordinate on the bottom point on the tether, t_x is the x -coordinate on the top, t_y is the y -coordinate on the top and b_y is the y -coordinate on the bottom, while χ was calculated using the y - and z -coordinates for the top and bottom tether marks, and ψ was calculated using the x - and z -coordinates for the left and right marks:

$$\begin{aligned}\eta &= \tan^{-1} \left(\frac{b_x - t_x}{t_y - b_y} \right) \\ \chi &= \tan^{-1} \left(\frac{b_y - t_y}{t_z - b_z} \right) \\ \psi &= \tan^{-1} \left(\frac{b_x - t_x}{t_z - b_z} \right).\end{aligned}\quad (1)$$

All angles were calculated relative to 0 deg in the respective plane of a locust generating stable flight without visual stimulation. For η , 0 deg was perpendicular to the midline of the locust when viewed from behind. For χ and ψ , 0 deg was directly in front of the locust as viewed from the side or above, respectively (Fig. 2).

EMG spike times were extracted by performing event detections on each trace and marking the peak within each event. Any incidence of double spikes was marked and imported along with single spike times into SigmaPlot (version 10.0, Systat Software, Richmond, CA, USA). Depressor asymmetry (DA) was calculated by subtracting the timing of the right m97 EMG (REMG) from the timing of the left m97 EMG (LEMG). Using this convention, a negative DA indicates that the LEMG fired before the REMG.

Observations of rotational angles showed that η consistently changed around 40 ms after an EMG spike (supplementary material Fig. S1). Changes in η were much clearer than those in ψ and χ , so were used as a standard for extracting all behavioural kinematic data (implying that it took ~40 ms after an EMG spike for a change in rotation to occur). This latency is similar to previously reported

behavioural reaction times in locusts responding to acoustic stimuli (see Boyan, 1985). Thus, values for ψ , χ and η were measured 40 ms after the timing of LEMG spikes when left turns occurred and REMG spikes when right turns occurred. These values were imported into SigmaPlot for further analysis. Left wing (θ_L) and right wing (θ_R) angles at the time of the forewing and hindwing downstroke were used to calculate wing asymmetries. This provided a negative value when $\theta_L > \theta_R$, which is indicative of attempted steering to the left (Robertson and Reye, 1992; Dawson et al., 2004b; Chan and Gabbiani, 2013).

Data from all animals were separated into discrete events and time aligned to TOC for graphing and correlation analysis (Fig. 2). For ψ , χ and η , these events were values recorded 40 ms after each EMG occurred. For all other data, such as forewing asymmetry (FWA), hindwing asymmetry (HWA), wingbeat frequency (WBF) and abdomen position (abdomen angle, ABD), events were extracted, by convention, at the time of LEMG spikes. Times and values of change in measured parameters were identified by selecting values outside of a 95% confidence interval (CI).

Statistical analysis

Statistical analysis was performed with SigmaStat 3.0 and plotted with SigmaPlot 10.0 (Systat Software). The timing and duration of behaviours were first tested for normality and equal variance. Parametric data were tested with a one-way ANOVA, whereas non-parametric data were tested with a Kruskal–Wallis ANOVA on ranks. A Tukey or Dunn's method *post hoc* multiple comparison was used to identify putative differences between measured parameters. Differences in the timing and values of changes in select measured parameters (DA, FWA, HWA, η , χ , ψ , WBF and ABD) for left and right turns were compared using a Student's t -test for parametric data and a Mann–Whitney rank sum test on non-parametric data.

Pearson product-moment correlation (PPM) was used to test for relationships between DA and other variables. By convention, we attributed a range of operational definitions to describe differences in the degree of correlation. PPM coefficient (r) values ranging from 0 to ± 0.09 were considered to not be correlated, where as values ranging from ± 0.1 to ± 0.29 , ± 0.3 to ± 0.49 , and ± 0.5 to ± 1 described variables that showed a small, medium or large correlation, respectively (Cohen, 1988). All significance was assessed at $P < 0.05$.

RESULTS

General behaviour

In straight flight, forewing movements on each side of the locust are symmetrical (Robertson and Reye, 1992; Santer et al., 2005) (see also supplementary material Movie 1). Following straight flight, most animals ($N=11$) performed a single behavioural response, while others performed two ($N=3$), three ($N=3$) or four ($N=1$) distinct behaviours during stimulus presentation. All animals either turned (left, $N=6$; right, $N=5$) or performed a glide ($N=7$) as an initial response to the looming stimulus. Animals that first responded with a turn did not show any additional responses before TOC whereas glides preceded up to three other behaviours. All animals turned as a final behaviour, irrespective of the preceding behaviour. Glides were followed by a left turn ($N=1$), a right turn ($N=2$), a stop followed by a left turn ($N=2$), another glide followed by a turn to the right ($N=1$), or another glide followed by a turn to the left then a turn to the right ($N=1$). Although our behavioural data show that flying locusts use different behaviours (and in different combinations) to avoid an approaching object during loosely tethered flight (see Chan and Gabbiani, 2013), we focused

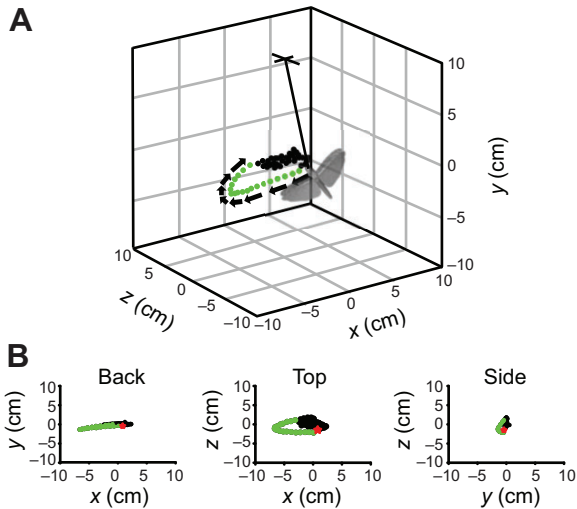


Fig. 3. Three-dimensional flight track of a locust performing an intentional steering manoeuvre in response to a lateral looming stimulus from the right. (A) Each dot represents real-world x -, y - and z -axis displacement coordinates extracted from the top tether mark during an entire 8 s video recording of a loosely tethered locust turning left. The locust image is scaled using real locust measurements from forewing tip to forewing tip and the black line leading to the locust represents the loose tether wire. Black dots represent positions during the pre-turn epoch and green dots represent positions during a turn. The position at the start of the turn is indicated by the locust image and the black arrows indicate the direction of motion. (B) Two-dimensional representations of the flight path from the rear, top and left side. Same colour scheme as in A, except that the position at the start of the turn is indicated by a red star. In A and B, note the relative consistency in free flight before the behaviour occurred, with deviations in the range of 6 cm from the mean in the epoch prior to the start of the turn. During the turn, the animal moved to the left, dropped in height and thrust forward. The point at which the animal changed trajectory back to centre is probably an effect of tethering (see Materials and methods).

our analysis on turns. Glides occurred relatively early during stimulus presentation (~ 1 s before TOC) and the changes we observed in measured parameters were most strongly associated with TOT. Using x -, y - and z -axis displacements we generated 3-dimensional flight path plots (see Fig. 3) that demonstrate consistency in free flight (prior to turning) and stereotypical turning responses to looming stimuli during loosely tethered flight.

Response time and duration

All observed avoidance behaviours occurred prior to TOC, with the earliest and latest occurring at -1.44 s (a glide) and -0.28 s (a turn), respectively (median of -0.740 s). Thus, we found a relatively wide range of behavioural response times [mean of -1.067 s for glides ($N=11$), -0.659 s for turns ($N=19$) and -0.600 s for stops ($N=2$)] (see Fig. 4A). There were no significant differences in the timing of turns (left or right) nor were stop initiation times different from turns, although all turns and stops occurred significantly later than glides ($F_{2,9.772}$, Tukey). Although turns that followed other behaviours tended to occur closer to TOC relative to turns that were the only behaviour performed, there were no differences in timing ($t_{17}=-2.086$).

The duration of each behaviour for each animal was calculated using frame-by-frame video analysis (see Materials and methods). Animals spent the longest time during a turn (~ 560 ms, $N=19$), followed by a glide (~ 120 ms, $N=9$) and then a stop (~ 40 ms, $N=2$) ($H_2=15.251$, Dunn's) (Fig. 4B). There were no significant differences in turn duration ($t_{17}=1.373$), regardless of whether another behaviour

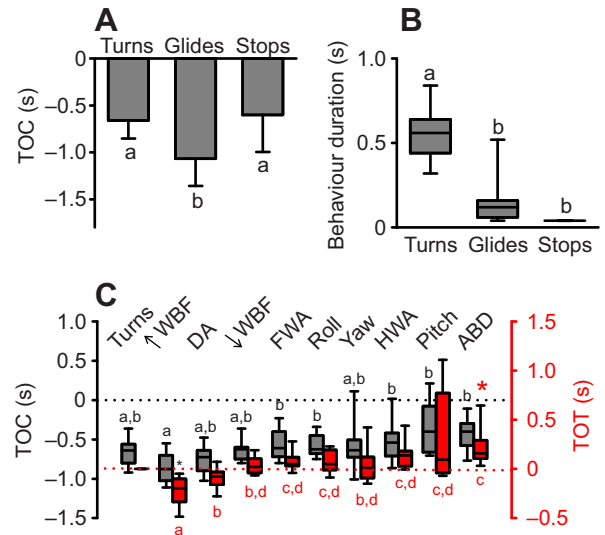


Fig. 4. Temporal properties of behavioural and kinematic parameters. (A) Initiation of turns ($N=19$), glides ($N=9$) and stops ($N=2$) relative to TOC. (B) Duration of turns ($N=19$), glides ($N=9$) and stops ($N=2$). (C) Time of change in behavioural, EMG, wing kinematic and body orientation parameters (see Materials and methods for description of data quantification). The left y-axis and grey boxes represent time relative to TOC (black dotted horizontal line). The right y-axis and red boxes represent time relative to TOT (red dotted horizontal line). Turn $N=19$, decrease in wing beat frequency (\downarrow WBF) $N=16$, EMG $N=19$, increase in wing beat frequency (\uparrow WBF) $N=18$, FWA $N=19$, η $N=19$, ψ $N=10$, χ $N=18$ and ABD $N=18$. Data in A are represented by their means \pm s.d., while data in B and C are represented by their medians with 10th, 25th, 75th and 90th percentiles. Different letters associated with each error bar denote significant differences between parameters. The red asterisk represents a value significantly different from TOT.

preceded a turn ($N=8$) or the turn was the only behaviour performed ($N=11$).

Behavioural parameters

To quantify the time and value of changes in different behavioural parameters, we aligned all data relative to TOC (Fig. 5A–H) and TOT (Fig. 5I–P). As a baseline value during straight flight, before a response to the stimulus (pre-turn epoch), data were averaged across a 1 s time interval from -4 to -3 s before TOC for each parameter from each animal ($N=18$) (Fig. 5). All data were separated based on turn direction (left, $N=10$; right, $N=9$) and baseline values were compared against the values that deviated outside a 95% CI (Fig. 6). Parameter values that exceeded the upper 95% CI were consistent with animals that turned right, while parameters that exceeded the lower 95% CI were consistent with animals that turned left. One animal performed a clear left and right turn during a single presentation; we decided to isolate the data for this animal into left and right comparisons, justified by quantifiable deviations above and below the 95% CI for measured parameters. We found no significant differences ($t_{17}=0.493$) when comparing the interval between the initiation of all left turns (-0.68 s, $N=10$) and right turns (-0.64 s, $N=9$) relative to TOC. Across all animals and measured parameters, there were no differences in the time when parameter changes exceeded the 95% CI based on turn direction (see below). Thus, we grouped all animals together regardless of turn direction when looking at the time of change, but isolated them based on direction for value at the time of change. Slight biases in the data

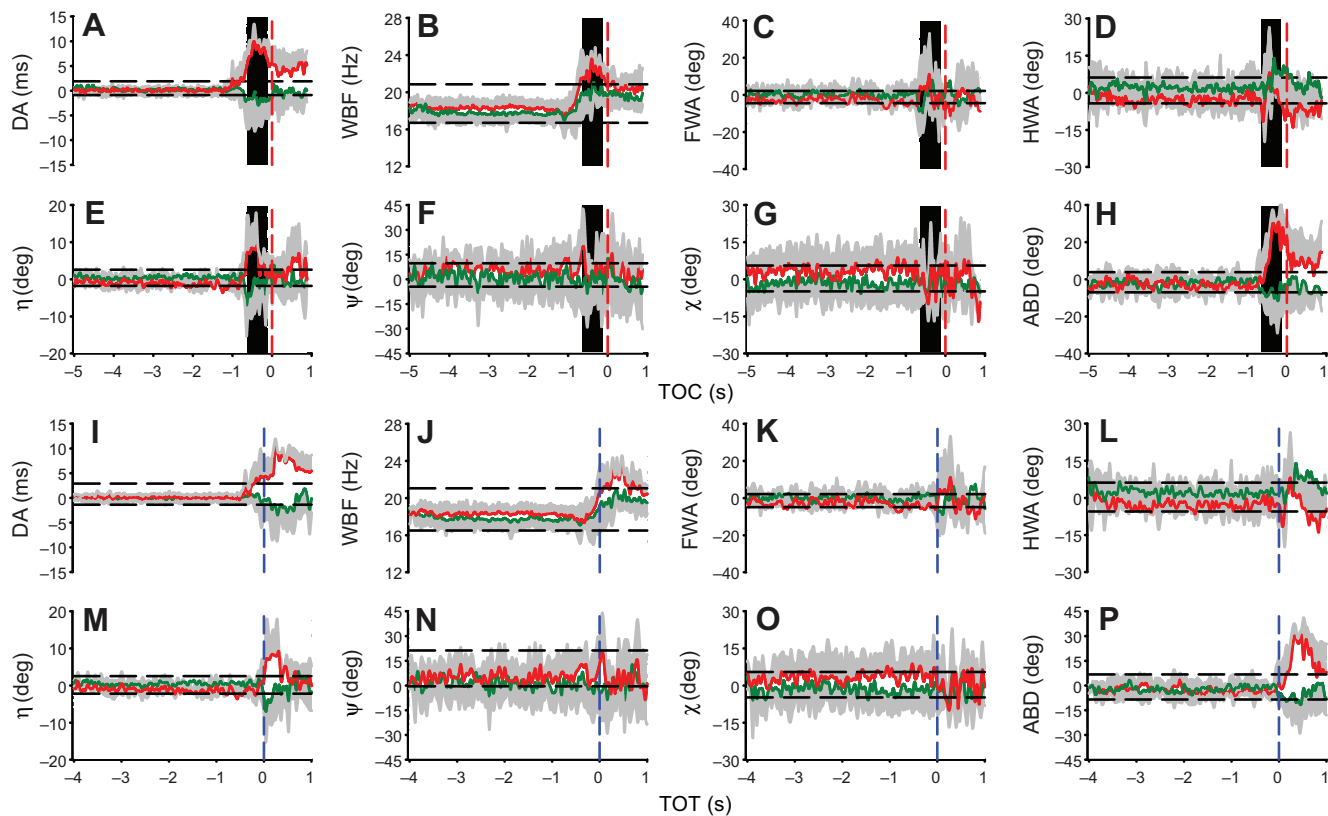


Fig. 5. Changes in depressor asymmetry (DA), FWA, HWA, ψ , χ and η angles, WBF and ABD over time for all animals ($N=18$). A–H are aligned to TOC, while I–P are aligned to TOT. Solid red lines represent mean values from animals that turned right (grey shading represents \pm s.d.) and solid green lines represent mean values from animals that turned left (grey shading represents \pm s.d.). For A–H, the vertical dashed red line represents TOC, black horizontal dashed lines represent the 95% confidence interval (CI) for the entire data set within the entire time window, and the solid black vertical bar represents the mean turning epoch. For I–P, a similar colour scheme and arrangement was used to that above, except that the blue vertical dashed line represents TOT.

were observed for most measured parameters. For example, most locusts ($N=12$) flew with a non-zero bias in FWA during the pre-turn epoch ($N=10$ were slightly negative and $N=2$ were slightly positive). However, these FWA biases did not influence turn direction as a similar number of animals turned in the same direction as the bias ($N=7$) to the number that turned in the opposite

direction to the bias ($N=5$). Moreover, $N=6$ locusts showed no bias in FWA ($N=3$ of those animals turned left and $N=3$ turned right). Biases among other behavioural parameters followed a similar trend, with the exception of ABD, where $N=11$ animals (61%) showed no bias, and η , where $N=10$ animals (56%) turned in the same direction as was reflected in the bias.

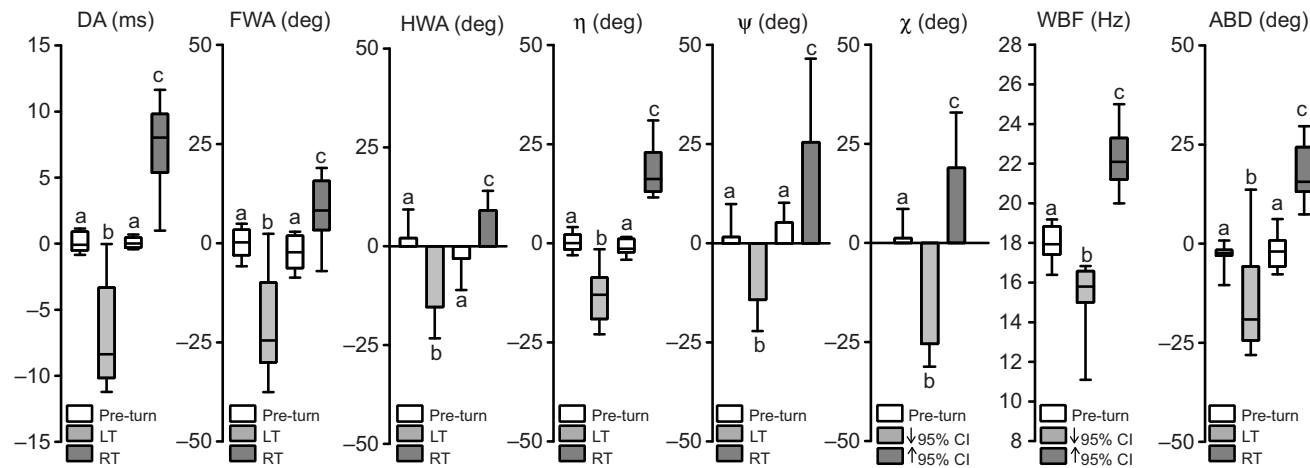


Fig. 6. Comparison of parameters during pre-turn and turning epochs for left and right turns. Each parameter is grouped based on left turns (LT) and right turns (RT), preceded by their respective pre-turn values. χ and WBF are arranged based on values that went below and above a 95% CI (see Results). Each box represents the median with 10th, 25th, 75th and 90th percentiles. Data for ψ and χ are represented by the mean \pm s.d./ \pm s.d. Different letters denote significant differences between parameters. DA (left $N=10$, right $N=9$), FWA (left $N=10$, right $N=9$), η (left $N=10$, right $N=9$), ψ (left $N=6$, right $N=4$), χ (below 95% CI $N=6$, above 95% CI $N=12$), WBF (below 95% CI $N=16$, above 95% CI $N=18$). For all pre-turn epoch values $N=18$.

Wing kinematics

We calculated mean (\pm s.d.) forewing and hindwing stroke amplitude from both wings from all animals (averaged from a minimum of 10 strokes during the pre-turn epoch) and found that the mean hindwing stroke amplitude (80.9 ± 7.3 deg) was higher than the mean forewing stroke amplitude (72.9 ± 7.8 deg). This relationship has been reported previously, albeit with larger amplitudes for each wing pair (Baker and Cooter, 1979). There was a clear variation in FWA around TOT (Fig. 5K). Frame-by-frame video analysis showed that around TOT, the forewings were typically asymmetric in all animals that turned (e.g. Fig. 1C). The left forewing (LFW) was depressed earlier than the right forewing (RFW) in the animals that turned left and the RFW was depressed earlier than the LFW in the animals that turned right. Pre-turn FWA values for left and right turns were not significantly different, but when changes in FWA occurred ~ 50 ms after TOT (Fig. 4C), they were significantly more negative for a left turn and positive for a right turn [$H_3=21.672$, Dunn's, LFWA ($N=10$), RFWA ($N=9$)] (Fig. 6). Furthermore, the time of FWA change was not different between left and right turns [LFWA ($N=10$) and RFWA ($N=9$), $t_{17}=0.847$]. While HWA was much more variable than FWA, most animals displayed clear deviations in HWA that went beyond a 95% CI before TOC (Fig. 5D) and after TOT (Fig. 5L). The timing of HWA changes for left and right turns was not significantly different [LHWA ($N=8$), RHWA ($N=6$), $t_{11}=1.007$]. Although pre-turn HWA values for left and right turns were not significantly different from each other, pre-turn HWA values were significantly different from changes in HWA during a turn, and left turn HWAs were significantly more negative than right turn HWAs [$F_3=14.825$, Dunn's, LHWA ($N=8$), RFWA ($N=6$)] (Fig. 6). We also found that changes in HWA were much later (although not significant) than changes in FWA, occurring at a median time of 140 ms after TOT (Fig. 4C).

For most animals ($N=14$) and for a single animal that turned twice, the WBF was below and above the 95% CI at two clear points (Fig. 5B,J). An increase in WBF (\downarrow WBF) occurred before TOT, while a decrease in WBF (\uparrow WBF) occurred around TOT. Based on turn direction, we found no differences in the timing of change [$L\downarrow$ WBF ($N=9$) versus $R\downarrow$ WBF ($N=7$), $t_3=28$; $L\uparrow$ WBF ($N=10$) versus $R\uparrow$ WBF ($N=9$), $t_{37}=98$] or value at the time of change [$L\downarrow$ WBF ($N=9$) versus $R\downarrow$ WBF ($N=7$), $t_{14}=-1.756$; $L\uparrow$ WBF ($N=10$) versus $R\uparrow$ WBF ($N=9$), $t_{17}=1.501$]. Thus, changes in WBF occurred regardless of turn direction and were subsequently analysed separately based on CI and not turn direction. We found that \downarrow WBF (16 Hz, $N=16$) was significantly lower and \uparrow WBF (22 Hz, $N=18$) was significantly higher than pre-turn values (18 Hz, $N=18$, $H_2=44.36$, Dunn's) (Fig. 6).

When aligned to TOT, changes in FWA occurred significantly later than changes in DA and \downarrow WBF ($H_8=44.38$, Dunn's). We also found that when aligned to TOT, \downarrow WBF occurred significantly earlier than any other parameter change and \uparrow WBF only differed from changes in ABD (Fig. 4C). These results suggest that a decrease in WBF is the first indication that a turning behaviour will occur. Following turn initiation, an increase in WBF occurs at the same time as a change in FWA that directly reflects the time and direction of a turn. Based on our data, we also suggest that HWA is not as predictive as FWA in estimating the direction and timing of a turn.

Body orientation

To examine changes in three rotational degrees of freedom (ψ , χ and η) before TOC, markers on the attached tether were used to calculate orientation angles using appropriate x -, y - and/or z -coordinates in 3-dimensional space. Fig. 5E–G and Fig. 5M–O

show changes in body position, time aligned to TOC and TOT, respectively, during object approach for all 18 animals. While data were more variable for ψ and χ , the η angle was relatively consistent throughout flight and showed pronounced positive or negative shifts before TOC and around TOT for all animals. Most animals ($N=10$) showed clear changes in ψ that deviated beyond the 95% CI around TOT. While pre-turn left and right η and ψ values were not different, values at the time of change were significantly different from pre-turn values and opposite to turn directions [$L\eta$ ($N=10$), $R\eta$ ($N=9$), $H_3=29.037$, Dunn's; $L\psi$ ($N=6$), $R\psi$ ($N=4$), $F_3=12.766$, Tukey] (Fig. 6). Based on turn direction, we found no differences in the timing of change for either η [$L\eta$ ($N=10$), $R\eta$ ($N=9$), $t_{56}=79$] or ψ [$L\psi$ ($N=6$), $R\psi$ ($N=4$), $t_8=0.909$] (Fig. 4C). While χ angles were overall quite low for both left and right turns compared with pre-turn values and opposite turns, no significant differences were found when compared across all animals [$L\chi$ ($N=9$), $R\chi$ ($N=9$), $H_3=2.524$]. However, when animals that showed deviations in χ above and below a 95% CI were analysed separately, TOT-associated values were clearly different from pre-turn values. χ angles below a 95% CI were significantly lower than pre-turn values [$L\chi$ ($N=6$), $R\chi$ ($N=6$), $F_3=36.99$] and the decrease was consistent between left and right turns (-25.8 ± 7.0 and -25.0 ± 4.9 , respectively). χ angles above a 95% CI were also significantly higher than pre-turn values [$L\chi$ ($N=3$), $R\chi$ ($N=3$), $F_3=7.016$], but were more variable (13.1 ± 3.4 and 24.9 ± 19.1 for left and turns, respectively). Thus, we analysed χ separate from turn direction (Fig. 6). We found all positive and negative shifts in χ were significantly higher and lower, respectively, than pre-turn values and relative to each other [pre-turn ($N=18$), negative changes ($N=12$), positive changes ($N=6$), $F_2=67.178$]. Although positive changes in χ tended to occur earlier and closer to TOT relative to negative changes, there were no significant differences in the timing of the decrease or increase ($t_{53}=40$).

These results show that changes in 3-dimensional rotational angles, specifically ψ and η , were associated with turning behaviour such that negative changes represented a left turn and positive changes represented a right turn. However, the timing of the change does not depend on turn direction. Moreover, χ was positive or negative regardless of turn direction, adding another layer of variability to the avoidance response.

Abdomen position

We quantified changes in abdomen position by analysing the magnitude of each shift related to the degree of deflection from the midline of the animal (see Materials and methods). Fig. 5H,P clearly shows changes in abdomen position, time aligned to TOC and TOT, during object approach for all 18 animals. We found no differences in pre-turn ABD for left or right turns, but when movement went beyond a 95% CI, ABD was significantly more negative during a left turn relative to that during a right turn [$LABD$ ($N=10$), $RABD$ ($N=8$), $H_3=20.613$, Dunn's] (Fig. 6). While the timing of abdominal position change for left and right turns was not significantly different [$LABD$ ($N=10$), $RABD$ ($N=9$), $t_{16}=0.616$], when aligned with TOT, movement occurred significantly later than a turn ($N=18$, $H_8=72.541$) (Fig. 4C). Therefore, although the direction of abdominal movement is related to steering direction, it is not associated with initiation of the turning behaviour.

Depressor muscle activity

Fig. 5A,I illustrates how the relative shift in the timing of left and right m97 spikes (DA) strongly reflects turn direction. During the pre-turn epoch DA is consistent, irrespective of impending turn direction. During turning, however, DA shifts were significantly

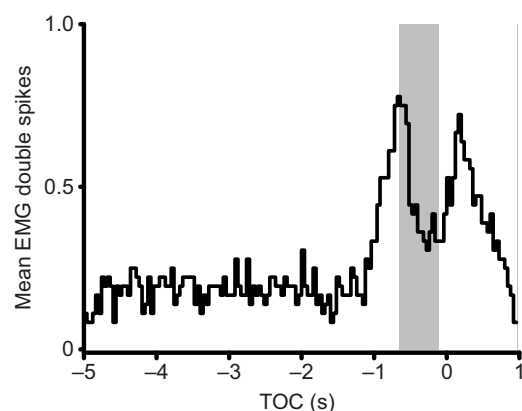


Fig. 7. Mean double spikes for all animals from both the left and right EMGs. The grey area shows the mean turning epoch. Double spikes were scored as either present (1) or absent (0). Thus, higher values indicate that double spikes occurred in more animals. The majority of double spiking increased prior to a turn, peaking shortly after initiation. There was a second peak after TOC and after the turns were completed that probably represents a compensatory response associated with a late tethering artefact (see Materials and methods).

more negative for left turns and positive for right turns [LEMG ($N=10$), REMG ($N=9$), $H_3=19.356$, Dunn's] (Fig. 6) before TOT and TOC (Fig. 4C). Although the relative sign values at the time of change were opposite for left and right turns, the number values were very consistent, displaying median latencies of -8.366 ms (minimum of -11.33 ms) and 8.034 ms (maximum of 11.65 ms) for LEMG and REMG, respectively. Changes in DA occurred at the same time regardless of turn direction [LEMG ($N=10$), REMG ($N=9$), $t_{17}=0.538$]. When aligned to TOT, changes in DA occurred significantly later than \downarrow WBF but earlier than changes in FWA, η , χ and abdomen movement ($N=19$, $H_8=72.541$). Previous studies showed that the m97 muscles are capable of firing single, double or triple spikes (Shoemaker and Robertson, 1998). We found that

single spiking occurred most often during straight flight and spiking stopped entirely during any cessation of flapping flight, such as a stop or glide. Most animals displayed a clear predominance of double spikes from both EMGs around TOT (Fig. 7) and generally before changes in FWA (Fig. 8). Further analysis of EMG traces revealed that preceding a turn most animals ($N=16$) consistently displayed an extra spike in the EMG on the inside of the turn relative to the EMG on the outside of the turn. These extra spikes typically preceded TOT by a single EMG cycle if TOT occurred between two EMG cycles; otherwise, the extra spike occurred at TOT (see Fig. 1C). The spike number ratio (outside:inside of turn) was 1:2 ($N=12$) or 2:3 ($N=4$). In one animal (see Fig. 2), the ratio was maintained as 0:1 where no spike was present in the REMG immediately preceding a turn to the left. These results strongly suggest that the relative timing of left and right m97 spikes and the ratio of spike number in the EMG on the inside of the turn affect turn timing and direction.

Correlations between muscles, wing kinematics and behaviour

We observed that DA, FWA and η appeared to change most strongly during a turn and were the most strongly correlated parameters that we measured (for example, see supplementary material Fig. S2). Changes in χ and WBF occurred regardless of the DA sign value and although abdomen movement reflects the sign value of DA it occurred later than TOT and thus is not correlated. Any change in HWA was also not correlated with any other parameter (data not shown). Thus, we examined putative relationships between DA and changes in FWA, ψ and η by performing a linear regression analysis on all data for each parameter from all animals ($N=18$). There were significant relationships between DA and FWA ($r=0.42$, $N=18$) and DA and η ($r=0.46$, $N=18$). However, DA and ψ showed no significant relationship ($r=0.05$, $N=18$). To determine whether changes in FWA predicted η and ψ , we performed a further regression analysis that revealed a significant correlation between FWA and η ($r=0.55$, $N=18$) but not between FWA and ψ ($r=0.08$,

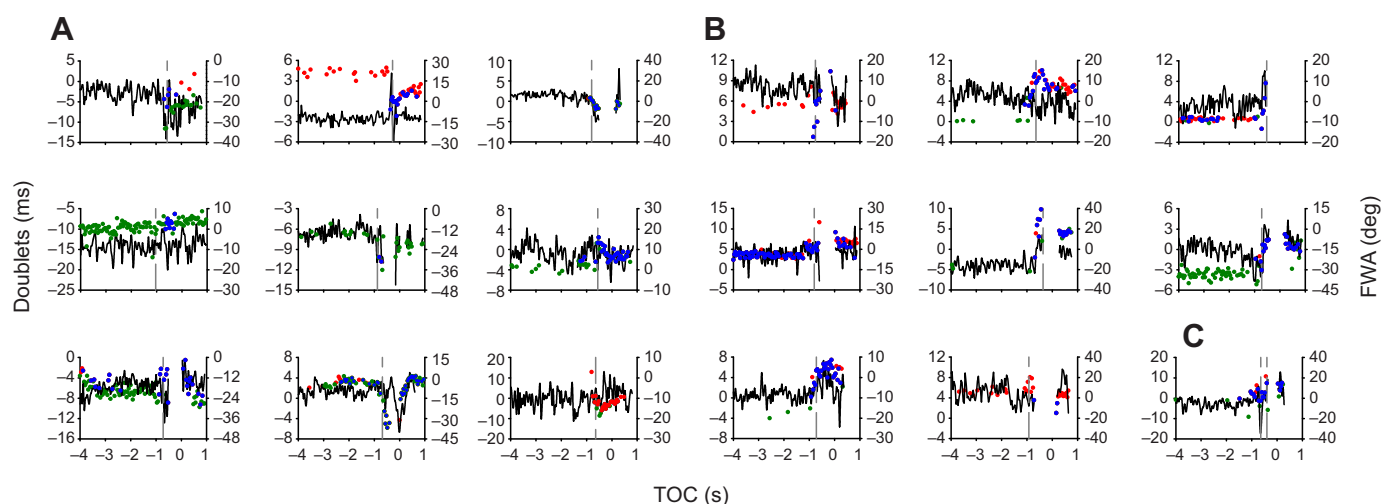


Fig. 8. EMG doublets recorded from the left and right m97 related to FWA for each locust. Within each panel, green dots represent LEMG double spikes, red dots represent REMG double spikes and blue dots indicate double spikes in both left and right EMGs (left axis). The solid black lines represent changes in FWA (right axis) and the dashed grey lines indicate TOT. (A) Nine animals that turned left. (B) Eight animals that turned right. (C) A single animal that performed a left turn followed by a right turn. Turns to the left or right generally occurred after the time of a change in DA and before the time of a change in FWA (negative for a left and positive for a right turn). Although double spiking occurred sporadically throughout flight, there was a general trend where both EMGs showed double spiking around the time of a turn. In addition, double spikes often occurred in EMGs on the inside of the turn (i.e. REMG for a right turn, LEMG for a left turn). Double spiking may be related to greater forewing depression, resulting in a turn to the direction where more spiking occurred.

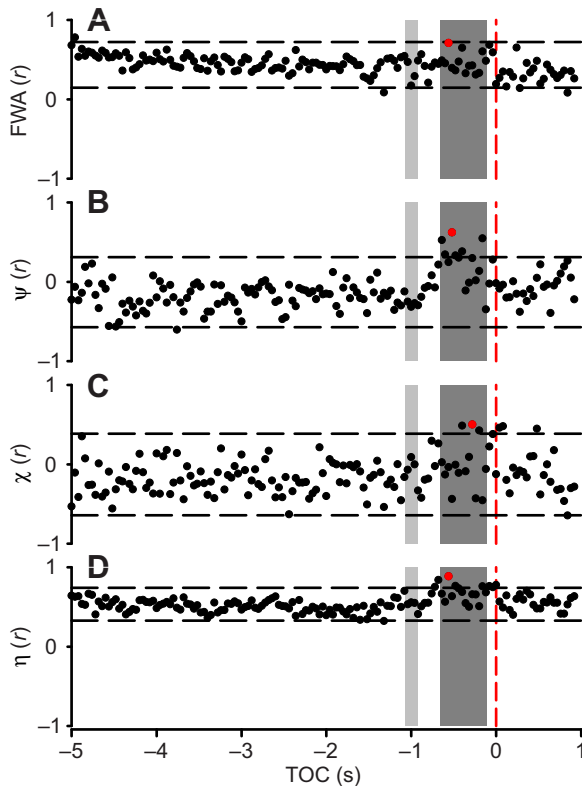


Fig. 9. Changes in correlation between DA and ψ , χ , η and FWA over time ($N=18$). Values were calculated 40 ms after a LEMG spike for left turns and REMG spike for right turns (see Materials and methods). Correlation between DA and all values became more positive as the object neared collision. Each black dot represents the Pearson product moment correlation coefficient between DA and FWA, ψ , χ or η for all 18 animals in a 40 ms time bin. The red dot represents the time of highest correlation. The two black dashed horizontal lines represent the 95% CI in each panel. The dotted red vertical line is TOC. Light grey bars represent the mean glide epoch ($N=9$) and dark grey bars represent the mean turning epoch ($N=19$). Although there should be no data points for the FWA during a glide, these are present because of the fact that the time of a glide was inconsistent between animals and the FWA data were compared in the same time frame from all animals. For all panels, significant changes in correlation occurred during the time of the turns, with changes in FWA, ψ and η occurring earlier than χ . The FWA (A) and η angle (D) showed an overall strong and consistent correlation with DA throughout flight that increased leading up to TOT and peaked during TOT. While correlations with ψ (B) and χ (C) angles were relatively weaker and more variable throughout flight, they also became more positive leading up to a maximum during a turn.

$N=18$). Although variability exists, the correlations between DA, FWA and η are medium to strong, while the correlation with ψ is small. Next, we examined how correlations changed over time (Fig. 9). DA for all 18 animals were time aligned to each rotational degree of freedom (ψ , χ and η) and FWA. Correlations between DA and these parameters increased and became more positive closer to TOC (Fig. 9) with the strongest correlations occurring with FWA and η . Moreover, the highest correlation values (above a 95% CI) over the entire stimulus presentation for all 18 animals and for all rotational degrees of freedom occurred during the time of a turn (Fig. 9). Although ψ and χ were also included in this analysis and displayed an increase in correlation, the coefficient values were low and less consistent than for FWA and η . Overall, these correlation analyses showed that DA is able to predict changes in FWA and,

ultimately, body rotation, especially η . Furthermore, even though ψ reflects sign changes in DA, those changes were not related to changes in DA or FWA.

DISCUSSION

Using a loosely tethered preparation, we show that while locusts generated variable, and sometimes multiple, responses when presented with a lateral looming object, most generated an intentional turn either toward or away from the object that was reflected in an alteration of bilateral timing of the downstroke of the forewings. We also found that steering was accompanied by \uparrow WBF and that abdomen movement during a turn occurred after the turn was initiated. Moreover, we describe, for the first time, that the relative timing and spike numbers in a flight depressor muscle (m97) can predict wing kinematics and 3-dimensional body orientation in locusts responding to looming stimuli.

Studying behavioural responses to looming stimuli in minimally restrained locusts, as described here (see also Chan and Gabbiani, 2013), provides a more natural representation of flight compared with experiments using rigidly tethered animals (Hedwig and Becher, 1998; Robertson and Reye, 1992; Robertson and Johnson, 1993; Gray et al., 2001; Santer et al., 2005; Santer et al., 2006; Simmons et al., 2010; Ribak et al., 2012). Using a combination of loose and more restrictive tight tethering, Chan and Gabbiani (Chan and Gabbiani, 2013) described wing kinematics and body positions in *Schistocerca americana*, which fly relatively short distances compared with the much longer flight durations of *L. migratoria*. Implantation of EMG electrodes required removal of the legs and thus could have affected steering behaviour given that ipsilateral hindleg extension has been implicated in collision-avoidance steering (Robertson and Reye, 1992). The additional mass and wind resistance of our tether design may also have affected steering behaviour. While our tether (20% body mass) was heavier than tethers used previously [12% body mass of *Schistocerca gregaria* (Kutsch et al., 1993)], preliminary studies using a weight-neutral loose tether attached to *L. migratoria* with legs removed (i.e. equivalent to an unloaded intact locust) (Mohr and Gray, 2003) showed similar types and timing of responses as reported here. Putative fulcrum effects notwithstanding, we observed behavioural durations (560 ms) consistent with those described previously [500 ms (Chan and Gabbiani, 2013)]. Moreover, our locusts generated stable free-flight postures and positions within a relatively small (48 cm³) 3-dimensional space during a pre-turn epoch (Figs 3, 5; supplementary material Fig. S3). Locusts were also able to perform steering manoeuvres, within a behaviourally relevant timeframe, that were correlated with stimulus parameters and wing muscle timing. Thus, we were able to examine parameters associated with turn initiation in full 3-dimensional space.

Rigidly tethered flying locusts consistently respond to lateral looming stimuli by interrupting flight and turning away from or toward the stimulus (Robertson and Johnson, 1993; Dawson et al., 1997; Robertson et al., 1996; Dawson et al., 2004b) and turning primarily away from the stimulus or performing a glide as a last ditch response (Robertson and Reye, 1992; Santer et al., 2005; Santer et al., 2006; Rind et al., 2008; Simmons et al., 2010; Santer et al., 2012; Ribak et al., 2012). We found that most animals turned as an initial response to the looming stimulus (33% turned left, 28% turned right), while 39% of the animals glided. Differences between our results and those reported earlier may be related to tethering conditions. Indeed, loosely tethered (Chan and Gabbiani, 2013) or freely flying (Dawson et al., 2004a) locusts show variable avoidance behaviours. Consistent with the concept that evasive behaviours are likely to be determined

by assessing the level of a threat (Schulze and Schul, 2001; Dawson et al., 2004a; Santer et al., 2005; Rosier, 2011; Chan and Gabbiani, 2013), we found that loosely tethered locusts performed a variety of behaviours in response to the same looming stimulus. Variability in avoidance responses to predatory attacks is a well-established concept (see Roeder, 1975). This variability could also be explained, at least in part, by the ability of the animal to manoeuvre in 3-dimensional space.

Gliding can occur close to TOT (Santer et al., 2005; Chan and Gabbiani, 2013) or precede a turn (Ribak et al., 2012). We also observed that glides preceded turns. However, these glides occurred relatively early in stimulus presentation (see Santer et al., 2005). Chan and Gabbiani (Chan and Gabbiani, 2013) reported glide frequencies as low as 7% in their loosely tethered experiments and, using a similar $l/|v|$ of 40 ms, Santer and colleagues (Santer et al., 2005) reported glide frequencies of 15%. Our glide frequency (37% of trials, $l/|v|=12$ ms) is consistent with studies using similar approach parameters where glide frequencies were as high as 46% [$l/|v|=6.7$ ms (Ribak et al., 2012)] or 80% [$l/|v|\leq 10$ ms (Santer et al., 2005)]. Moreover, our glide durations (140 ms) are consistent with those reported by Santer and colleagues (137 ms) (Santer et al., 2005). They (Santer et al., 2005) reported that following a glide, animals increased their WBF (also similar to our findings, where \uparrow WBF is associated with TOT and not a glide) or folded their wings (similar to a stop). Ribak and colleagues (Ribak et al., 2012) proposed that gliding may be a preparation for a turn. Indeed, we show that glides occur significantly earlier than stops and turns, with the last two behaviours occurring around the same time (Fig. 4A). Further investigation is required to identify whether glides are part of a preparatory response for avoidance or are a separate behaviour. Given that locusts generate glides either when presented with stimuli modelled from videos of swarms (Santer et al., 2012) or within actual swarm conditions (Baker and Cooter, 1979), it is likely that gliding may be an important strategy for collision avoidance. While findings to date have not been able to describe detailed temporal properties of gliding in the wild, our data suggest that glides are part of a suite of behaviours rather than a stereotyped final emergency response to looming.

Contrary to earlier studies describing turns, or indications of turns, showing locusts moving away from the stimulus in free flight (Dawson et al., 2004a) or tethered (Robertson and Johnson, 1993; Dawson et al., 1997; Santer et al., 2005; Santer et al., 2012; Ribak et al., 2012), we found approximately equal incidences of turning toward or away from the looming disc. Turn direction variability was also reported for responses to visual (Chan and Gabbiani, 2013) and thermal (Shoemaker and Robertson, 1998) stimuli. Escape variability may be a way to preclude anticipation by predators (Card, 2012) and is a common strategy employed by many animals (Domenici et al., 2011).

Response times reported here are less variable and occurred >200 ms earlier than those reported by Chan and Gabbiani (Chan and Gabbiani, 2013), whereas turn initiation preceded body rotation changes by ~50 ms (based on median ψ and η changes), which is consistent with other findings (Ribak et al., 2012; Chan and Gabbiani, 2013). While different response times may be related to different approach parameters used in these studies, our findings are consistent in that locusts are able to generate significant 3-dimensional body rotations within one wing beat (see supplementary material Movie 1) (see also Dawson et al., 2004b).

Cessation of flight (stops) occurs in many insects responding to threatening stimuli, (Miller and Surlykke, 2001; Dawson et al., 2004a; Santer et al., 2005; Rind et al., 2008) and results in a rapid

decrease in altitude. We found that stops were relatively brief, lasting ~40 ms, and typically preceded resumption of flapping and a turn. While stops resulted in a decrease in altitude (see supplementary material Fig. S3), the constraints of our tether limited the extent of the decrease and thus may have triggered resumption of flapping.

Previously studies describing either ψ and χ (Robertson and Johnson, 1993) or η (Ribak et al., 2012) showed that changes in ψ and η reflect flight steering direction. Although we also found that the ψ angle reflected turn direction, it was relatively more variable than η , which was most strongly related with a turn and was consistent among all animals (Figs 5, 6). While changes in WBF could induce variability in ψ (see Robertson and Johnson, 1993), the timing of changes in ψ and η were consistent relative to TOT (Fig. 4), as was the amplitude change (from ~0 deg pre-turn to ± 20 deg during the turn). The predominance of decreased χ values associated with steering that we observed (67%) is contrary to a predominance of positive χ changes reported by Chan and Gabbiani (Chan and Gabbiani, 2013). This difference may be explained by the relative stability of flight orientation during straight flight observed here for *L. migratoria*.

We observed wingbeat frequencies that are within the range of previous reports from rigidly tethered locusts (Robertson and Johnson, 1993; Shoemaker and Robertson, 1998; Santer et al., 2005). We found that during minimally restrained flight, \downarrow WBF occurred before a turn and \uparrow WBF occurred during a turn (see Fig. 6; supplementary material Movie 1). A similar decrease in WBF has been shown to precede turns (Ribak et al., 2012) and glides (Santer et al., 2005) whereas tethered (Robert, 1989; Dawson et al., 1997) and free-flying (Dawson et al., 2004a) locusts have been shown to increase WBF, and thus flight speed, as turns were completed. \downarrow WBF may be part of a preparatory response before initiating a turn as it consistently occurs significantly earlier than TOT. While \downarrow WBF may also be a preparation for a glide in rigidly tethered locusts (Santer et al., 2005), the time of our \downarrow WBF was significantly earlier than TOT but not glides ($F_2=11.245$, Tukey). Therefore, we suggest that \downarrow WBF is more related to turning behaviour in locusts that are able to manoeuvre in 3-dimensional space and that \uparrow WBF may be a compensatory response to lost altitude during the turn or a mechanism to regain lift and stabilize flight (Santer et al., 2005; Ribak et al., 2012).

Although our FWA shifted negatively for left turns and positively for right turns, the magnitude of the shift was often variable as it was sometimes relative to a non-zero pre-turn baseline (see Robertson and Reye, 1992; Robertson and Johnson, 1993; Shoemaker and Robertson, 1998). The bias in FWA, similar to other biases in measure parameters, did not influence turn direction as there was a near-equal number of animals that turned in the direction of the FWA bias, turned in the opposite direction to the FWA bias, and turned in either direction with no bias in FWA ($N=7$, 5 and 6, respectively). Using a similar $l/|v|$ of 12 ms, Robertson and Johnson (Robertson and Johnson, 1993) reported asymmetries of ~15 deg during attempted steering, which matches what we observed. We also found that FWA developed ~50 ms after TOT (Fig. 4C), consistent with previous descriptions of asymmetries developing during the downstroke of the wing beat when locusts are attempting to steer (Robertson and Reye, 1992).

Earlier studies using rigidly tethered (Robertson and Johnson, 1993; Shoemaker and Robertson, 1998), minimally restrained (Chan and Gabbiani, 2013), or free-flying locusts (Dawson et al., 2004a) found little to no change in HWA during a turn. While we found that HWA reflected turn direction (Fig. 4C, Fig. 5), changes in HWA occurred well after TOT. Ribak and colleagues (Ribak et al., 2012)

recently reported that hindwing pronation is important for turning, contributing to η . As we were unable to measure wing pronation in our experiments, we cannot confirm that either forewing or hindwing pronation is associated with flight steering in animals free to manoeuvre in 3-dimensional space.

Shifts in abdomen position have been described as a component of intentional flight steering (Robert, 1989; Robertson and Johnson, 1993; Gray et al., 2001), where elevation and shifting to the inside of the turn occurs at the same time as extension of the hindleg on the inside of the turn (Robertson and Johnson, 1993). The results of these movements are thought to shift the locust's centre of mass to initiate a turn (Robertson and Reye, 1992). While we observed shifts in abdomen orientation associated with the direction of the turn, this change occurred after turn initiation. Taken together with the fact that turns can occur in one wing beat, we suggest that rotation of the centre of mass is produced by aerodynamic forces established by FWA and that abdominal movement may be a result of delayed inertial forces produced by the turn. Alternatively, movement of the abdomen may be slightly delayed as its involvement is in turn completion not initiation.

Changes in DA, in addition to the presence/absence of EMG spikes, can predict changes in FWA, which in turn predicts whole-body movements. The values we report of DA related to turn initiation are consistent with those previously reported for m97 in response to acoustic stimuli (Dawson et al., 1997; Dawson et al., 2004b). Consistent with Shoemaker and Robertson (Shoemaker and Robertson, 1998) we found that most double spiking occurred around TOT (Figs 7, 8). We also observed that at TOT, the ratio of LEMG and REMG spike number reflected turn direction, where most animals showed one additional spike on the EMG on the inside of the turn (see Fig. 1C for example), represented as a double, triple or in one case a single spike. The single spike occurred when a spike was 'dropped' in the opposite EMG (see Fig. 2) (Dawson et al., 2004b). The presence of the extra spike on the inside of a turn may indicate greater force associated with earlier depression whereas the absence of a spike on the outside of a turn may result in a relatively faster elevation, either of which could be involved in developing an asymmetry. Correlation analysis showed that DA is a good predictor of FWA and η (Figs 9, 10) and that correlations peak during TOT (Fig. 9). Moreover, DA was not related to gliding or stopping. We also show that FWA is strongly correlated with η and weakly correlated with ψ and HWA (for example, see supplementary material Fig. S2). This finding differs from that of Chan and Gabbiani, though they did not measure η (Chan and Gabbiani, 2013).

Future experiments using a variety of stimuli are needed to address whether locusts use different levels of threat assessment to perform different behaviours. Chan and Gabbiani (Chan and Gabbiani, 2013) suggest that selection of avoidance behaviour (fast or slow and direction) depends on the position of the locust relative to the looming stimulus. However, we did not observe any relationship between the position of the locust and the direction of turn, and deviations during stable flight (see Fig. 3) were very small and probably did not affect turn direction. Nevertheless, selection of the most suitable behaviour for avoidance probably depends on the dynamics of the sensory environment. Thus, it would be important to test the effects of more dynamic visual environments, such as flow fields, variation in $l/|v|$ values, or more complex trajectories, which have previously been shown to influence the response of a motion-sensitive neural circuit implicated in collision avoidance (McMillan and Gray, 2012).

We propose an initial model of the timing and relationships between parameters associated with flight steering that account for

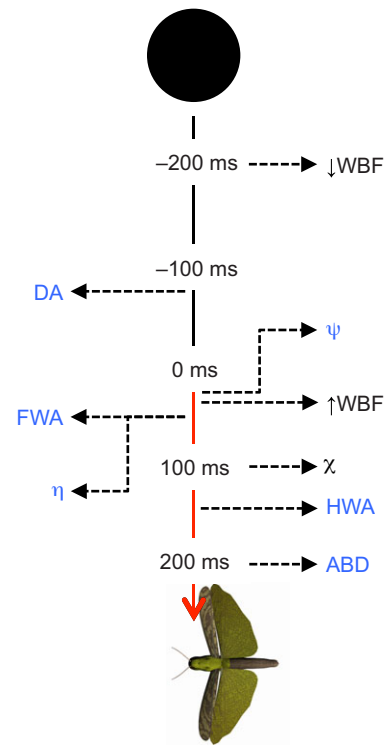


Fig. 10. Proposed behavioural model representing an avoidance turn in response to a lateral looming stimulus. The arrow represents part of the pre-turn epoch (black) and post-turn epoch (red) over 500 ms. The black dashed arrows indicate the time of change for each parameter (see Results). We calculated the linear regression coefficient (r) and equation of the line describing the relationship between DA and FWA ($r=0.42$, $y=0.97x-5.72$), DA and η ($r=0.46$, $y=0.73x+1.36$), and FWA and η ($r=0.55$, $y=0.31x-8.42$). Parameters on the left side of the arrow show medium to high correlations with each other, while parameters on the right side share no predictable relationship. All parameters in blue share a matching sign value during a turn (i.e. negative for a left and positive for a right turn).

depressor muscle activity, wing kinematics and body orientation in 3-dimensional space (Fig. 10). The first indication of a turn is \downarrow WBF that occurs prior to TOT. Approximately 70 ms before TOT, DA develops. Once a turn is initiated, ψ changes followed by \uparrow WBF. At this point, the change in DA is at a maximum and causes a shift in FWA that changes the η angle within a few milliseconds. Finally there is a change in χ , followed by a change in HWA and abdominal ruddering. Changes in WBF and χ occur regardless of turn direction; however, DA, FWA, HWA, ψ , η and ABD all reflect turn direction. Separating the parameters further, changes in ψ , HWA and ABD are independent of changes in DA, based on the time of changes and weak correlations. Based on the equation of the linear regression line (Fig. 10) we can predict changes in FWA and η angle using DA. This prediction will be used in computer-generated closed-loop experiments to provide appropriate visual feedback during flight steering while recording from suites of flight muscles and multiple motion-sensitive visual neurons (Gray et al., 2010), allowing for an unprecedented understanding of the neural mechanisms of adaptive behaviour in this model system.

LIST OF SYMBOLS AND ABBREVIATIONS

ABD	abdomen angle
CI	confidence interval
DA	depressor asymmetry (LEMG – REMG)
EMG	electromyography

FWA	forewing asymmetry
HWA	hindwing asymmetry
<i>l</i>	half size of the object
LEMG	left electromyography
LFW	left forewing
REMG	right electromyography
RFW	right forewing
TOC	time of projected collision
TOT	time of turn
<i>v</i>	absolute approach velocity
WBF	wingbeat frequency
↑WBF	increase in WBF
↓WBF	decrease in WBF
η	roll
θ _L	left wing angle
θ _R	right wing angle
χ	pitch
ψ	yaw

ACKNOWLEDGEMENTS

We thank I. Benaragama, E. Bokshowan and K. Hunter for technical assistance and preliminary data analysis.

AUTHOR CONTRIBUTIONS

G.A.M. analyzed the data, interpreted the results, prepared the figures, and wrote and revised the manuscript; V.L. performed the experiments; J.R.G. conceived and designed the experiments, interpreted the results, revised the manuscript, and approved the final version of the manuscript.

COMPETING INTERESTS

No competing interests declared.

FUNDING

Funding was provided by the Natural Sciences and Engineering Research Council of Canada, the Canada Foundation for Innovation, and the University of Saskatchewan.

REFERENCES

- Baker, P. S. and Cooter, R. J. (1979). The natural flight of the migratory locust, *Locusta migratoria* L. I. Wing movements. *J. Comp. Physiol. A* **131**, 79-87.
- Baker, P. S., Gewecke, M. and Cooter, R. J. (1981). The natural flight of the migratory locust, *Locusta migratoria* L. III. Wing-beat frequency, flight speed and attitude. *J. Comp. Physiol. A* **141**, 233-237.
- Boyan, B. S. (1985). Auditory joint input to the flight system of the locust. *J. Comp. Physiol. A* **156**, 79-91.
- Burrows, M. (1995). Motor patterns during kicking movements in the locust. *J. Comp. Physiol. A* **176**, 289-305.
- Burrows, M. and Rowell, C. H. F. (1973). Connections between descending visual interneurons and metathoracic motoneurons in the locust. *J. Comp. Physiol. A* **85**, 221-234.
- Card, G. M. (2012). Escape behaviors in insects. *Curr. Opin. Neurobiol.* **22**, 180-186.
- Chan, R. W. and Gabbiani, F. (2013). Collision-avoidance behaviors of minimally restrained flying locusts to looming stimuli. *J. Exp. Biol.* **216**, 641-655.
- Cohen, J. (1988). *Statistical Power Analysis For The Behavioral Sciences*, 2nd edn. Hillsdale, NJ: Erlbaum.
- Dawson, J. W., Dawson-Scully, K., Robert, D. and Robertson, R. M. (1997). Forewing asymmetries during auditory avoidance in flying locusts. *J. Exp. Biol.* **200**, 2323-2335.
- Dawson, J. W., Kutsch, W. and Robertson, R. M. (2004a). Auditory-evoked evasive manoeuvres in free-flying locusts and moths. *J. Comp. Physiol. A* **190**, 69-84.
- Dawson, J. W., Leung, F. H. and Robertson, R. M. (2004b). Acoustic startle/escape reactions in tethered flying locusts: motor patterns and wing kinematics underlying intentional steering. *J. Comp. Physiol. A* **190**, 581-600.
- Domenici, P., Blagburn, J. M. and Bacon, J. P. (2011). Animal escapology II: escape trajectory case studies. *J. Exp. Biol.* **214**, 2474-2494.
- Fotowat, H., Fayyazuddin, A., Bellen, H. J. and Gabbiani, F. (2009). A novel neuronal pathway for visually guided escape in *Drosophila melanogaster*. *J. Neurophysiol.* **102**, 875-885.
- Fotowat, H., Harrison, R. R. and Gabbiani, F. (2011). Multiplexing of motor information in the discharge of a collision detecting neuron during escape behaviors. *Neuron* **69**, 147-158.
- Gaten, E., Huston, S. J., Dowse, H. B. and Matheson, T. (2012). Solitary and gregarious locusts differ in circadian rhythmicity of a visual output neuron. *J. Biol. Rhythms* **27**, 196-205.
- Gray, J. R., Lee, J. K. and Robertson, R. M. (2001). Activity of descending contralateral movement detector neurons and collision avoidance behaviour in response to head-on visual stimuli in locusts. *J. Comp. Physiol. A* **187**, 115-129.
- Gray, J. R., Blinco, E. and Robertson, R. M. (2010). A pair of motion-sensitive neurons in the locust encode approaches of a looming object. *J. Comp. Physiol. A* **196**, 927-938.
- Hassenstein, B. and Huster, R. (1999). Hiding responses of locusts to approaching objects. *J. Exp. Biol.* **202**, 1701-1710.
- Hedwig, B. and Becher, G. (1998). Forewing movements and intracellular motoneurone stimulation in tethered flying locusts. *J. Exp. Biol.* **201**, 731-744.
- Holmqvist, M. H. and Srinivasan, M. V. (1991). A visually evoked escape response of the housefly. *J. Comp. Physiol. A* **169**, 451-459.
- Horridge, G. A. and McLean, M. (1978). The dorsal eye of the mayfly *Atalophlebia* (Ephemeroptera). *Proc. R. Soc. B* **200**, 137-150.
- Kutsch, W., Schwarz, G., Fischer, H. and Kautz, H. (1993). Wireless transmission of muscle potentials during free flight of a locust. *J. Exp. Biol.* **185**, 367-373.
- Liu, Y.-J., Wang, Q. and Li, B. (2011). Neuronal responses to looming objects in the superior colliculus of the cat. *Brain Behav. Evol.* **77**, 193-205.
- McMillan, G. A. and Gray, J. R. (2012). A looming-sensitive pathway responds to changes in the trajectory of object motion. *J. Neurophysiol.* **108**, 1052-1068.
- Miall, R. C. (1978). The flicker fusion frequencies of six laboratory insects, and the response of the compound eye to mains fluorescent 'ripple'. *Physiol. Entomol.* **3**, 99-106.
- Miller, L. A. and Surlykke, A. (2001). How some insects detect and avoid being eaten by bats: Tactics and counter-tactics of prey and predator. *Bioscience* **51**, 570-581.
- Möhl, B. and Zarnack, W. (1977a). Activity of the direct downstroke flight muscles of *Locusta migratoria* L. during steering behavior in flight. II. Dynamics of the time shift and changes in burst length. *J. Comp. Physiol. A* **118**, 235-247.
- Mohr, N. A. and Gray, J. (2003). Collision avoidance responses in loosely tethered flying locusts. *Neurosci. Abstr.* Program number 403.20.
- Nakagawa, H. and Hongjian, K. (2010). Collision-sensitive neurons in the optic tectum of the bullfrog, *Rana catesbeiana*. *J. Neurophysiol.* **104**, 2487-2499.
- Oliva, D., Medan, V. and Tomsic, D. (2007). Escape behavior and neuronal responses to looming stimuli in the crab *Chasmagnathus granulatus* (Decapoda: Grapsidae). *J. Exp. Biol.* **210**, 865-880.
- Ribak, G. R., Rand, D., Weihs, D. and Ayali, A. (2012). Role of wing pronation in evasive steering of locusts. *J. Comp. Physiol. A* **198**, 541-555.
- Rind, F. C., Santer, R. D. and Wright, G. A. (2008). Arousal facilitates collision avoidance mediated by a looming sensitive visual neuron in a flying locust. *J. Neurophysiol.* **100**, 670-680.
- Robert, D. (1989). The auditory behaviour of flying locusts. *J. Exp. Biol.* **147**, 279-301.
- Robertson, R. M. and Johnson, A. G. (1993). Collision avoidance of flying locusts: steering torques and behaviour. *J. Exp. Biol.* **183**, 35-60.
- Robertson, R. M. and Reye, D. N. (1992). Wing movements associated with collision-avoidance manoeuvres during flight in the locust *Locusta migratoria*. *J. Exp. Biol.* **163**, 231-258.
- Robertson, R. M., Kuhnert, C. and Dawson, J. W. (1996). Thermal avoidance during flight in the locust *Locusta migratoria*. *J. Exp. Biol.* **199**, 1383-1393.
- Roeder, K. D. (1975). Neural factors and evitability in insect behavior. *J. Exp. Zool.* **194**, 75-88.
- Rosier, R. L. (2011). Behavior under risk: how animals avoid becoming dinner. *Nature Education Knowledge* **2**, 8.
- Santer, R. D., Simmons, P. J. and Rind, F. C. (2005). Gliding behaviour elicited by lateral looming stimuli in flying locusts. *J. Comp. Physiol. A* **191**, 61-73.
- Santer, R. D., Rind, F. C., Stafford, R. and Simmons, P. J. (2006). Role of an identified looming-sensitive neuron in triggering a flying locust's escape. *J. Neurophysiol.* **95**, 3391-3400.
- Santer, R. D., Rind, F. C. and Simmons, P. J. (2012). Predator versus prey: locust looming-detector neuron and behavioural responses to stimuli representing attacking bird predators. *PLoS ONE* **7**, e50146.
- Schulze, W. and Schulz, J. (2001). Ultrasound avoidance behaviour in the bushcricket *Tettigonia viridissima* (Orthoptera: Tettigoniidae). *J. Exp. Biol.* **204**, 733-740.
- Shoemaker, K. and Robertson, R. M. (1998). Flight motor patterns of locusts responding to thermal stimuli. *J. Comp. Physiol. A* **183**, 477-488.
- Simmons, P. J. (1980). Connexions between a movement-detecting visual interneurone and flight motoneurons of a locust. *J. Exp. Biol.* **86**, 87-97.
- Simmons, P. J., Rind, F. C. and Santer, R. D. (2010). Escapes with and without preparation: the neuroethology of visual startle in locusts. *J. Insect Physiol.* **56**, 876-883.
- Straw, A. D. (2008). Vision egg: an open-source library for realtime visual stimulus generation. *Front. Neuroinform.* **2**, 4.
- Sztarker, J. and Tomsic, D. (2008). Neuronal correlates of the visually elicited escape response of the crab *Chasmagnathus* upon seasonal variations, stimuli changes and perceptual alterations. *J. Comp. Physiol. A* **194**, 587-596.
- Waloff, Z. (1972). Orientation of flying locusts, *Schistocerca gregaria* (Forsk.), in migrating swarms. *Bull. Entomol. Res.* **62**, 1-72.
- Wang, Y. and Frost, B. J. (1992). Time to collision is signalled by neurons in the nucleus rotundus of pigeons. *Nature* **356**, 236-238.
- Zarnack, W. (1988). The effect of forewing depressor activity on wing movement during locust flight. *Biol. Cybern.* **59**, 55-70.